JOURNAL OF Applied Polymer SCIENCE

Enhancement of the Antibacterial Activity of Natural Rubber Latex Foam by the Incorporation of Zinc Oxide Nanoparticles

W. G. I. U. Rathnayake,[1] H. Ismail,[1] A. Baharin,[2] I. M. C. C. D. Bandara,[3] Sanath Rajapakse[3]

[1]School of Materials and Mineral Resources Engineering, Universiti Sains Malaysia, Penang, Malaysia

[2]School of Industrial Technology, Universiti Sains Malaysia, Penang, Malaysia

[3]Department of Molecular Biology and Biotechnology, Faculty of Science, University of Peradeniya, Peradeniya, Sri Lanka

Correspondence to: H. Ismail (E-mail: hanafi@eng.usm.my)

ABSTRACT: The synthesis and characterization of ZnO-nanoparticle-incorporated natural rubber latex foam (NRLF) are described in this article. ZnO nanoparticles were added as the primary gelling agent by the replacement of the microsized ZnO particles, whereas the control sample of the NRLF was made without the addition of any ZnO particles. ZnO nanopowder was evaluated by X-ray diffraction (XRD), whereas the aqueous dispersion of nano-ZnO was evaluated by transmission electron microscopy (TEM) micrograph analysis. The modified NRLF materials were evaluated by scanning electron microscopy (SEM)–energy-dispersive X-ray (EDX) analysis and XRD analysis. The antibacterial activities of the modified NRLF samples were evaluated quantitatively and qualitatively by antibacterial susceptibility tests against Gram-positive *Staphylococcus aureus* and Gram-negative *Escherichia coli* bacteria. We found that the XRD peaks matched perfectly with reference code 98-002-6593, which was the hexagonal phase. The particle sizes given by TEM image analysis were less than 60 nm. Most of the XRD peaks obtained for the modified NRLF matched with that of the ZnO nanopowder; this proved the presence of nano-ZnO in the modified NRLF. Further, it was proven by SEM and EDX analysis. The NRLF modified by nanosized ZnO inhibited the growth of the so-called bacteria in a very strong manner. © 2013 Wiley Periodicals, Inc. J. Appl. Polym. Sci. **2014**, *131*, 39601.

KEYWORDS: elastomers; foams; nanoparticles; nanowires and nanocrystals; rubber; synthesis and processing

Received 21 March 2013; accepted 30 May 2013

DOI: 10.1002/app.39601

INTRODUCTION

Metals and metal oxides have been well-known antimicrobial agents for a very long time.[1] Among the many types of antimicrobial metal and metal oxide nanoparticles, including silver, gold, aluminum, TiO_2, MgO, and CuO nanoparticles,[2] ZnO nanoparticles are a well-known and very prominent antimicrobial metal oxide because of their spectacular properties.[3] Although the antibacterial mechanism of ZnO is still under investigation, ZnO nanomaterials present good antimicrobial activity in various applications and products.[4–9] Sawai et al.[10] found that the most important mechanism for killing microorganisms by ZnO was the production of hydrogen peroxide (H_2O_2) from the photocatalytic generation. Some studies have also found that the production of reactive oxygen species (ROS) by ZnO nanoparticles could interact with the bacterial cells and cause the death of the cells.[11,12] Brayner et al.[13] and Huang et al.[14] reported that the diffusion of ZnO through the cell cover and disorganization of the bacterial membrane upon contact with ZnO nanoparticles could reduce bacterial growth. Another mechanism for killing microorganisms is the larger accumulation of the nanoparticles within the cell membrane and cytoplasm.[15]

ZnO is also a widely used semiconductor-type metal oxide in rubber and rubber-related industries as a curing activator in sulfur-curing vulcanization systems.[16] ZnO is also used as a preservative agent for centrifuged natural rubber latex (NRL).[17–20] In the synthesis of natural rubber latex foam (NRLF) by the Dunlop method, ZnO is used as the primary gelling agent.[21,22] Not only in rubber industries but also in other industries such as paint and coatings, cosmetics, textiles, pharmaceuticals, plastics, batteries, semiconductor devices, and solar cells is ZnO used very extensively.[23] The use of ZnO to impart antimicrobial activities to various kinds of materials is an increasing research area among many fields, including polymeric materials,[8] textiles,[5,7,9,24] and the medical field,[25] and also in the production of some medicines.[26]

In the NRLF manufacturing process by the Dunlop manufacturing method, microsized ZnO together with diphenylguanidine (DPG) are used as the primary gelling agent to gel unvulcanized

Table I. Formulation of the NRL Compounds for the Synthesis of the NRLF Samples by the Dunlop Process

	Dry pphr			
	Preparation of ZnO-nanoparticle-incorporated NRLF		Preparation of the control NRLF	
Ingredient	4-pphr Micro-ZnO (sample C)	2-pphr Nano-ZnO (sample D)	Control sample (without ZnO)	4-pphr Microsized ZnO (sample B)
60% NRL	100.00	100.00	100.00	100.00
20% Potassium oleate soap	2.00	2.00	2.00	2.00
50% Sulfur	2.50	2.50	2.50	2.50
50% Phenolic-type antioxidant	1.00	1.00	1.00	1.00
50% ZMBT	1.00	1.00	1.00	1.00
50% ZDEC	1.00	1.00	1.00	1.00
40% ZnO nanopowder	4.00	2.00	0.00	0.00
40% DPG	0.30	0.30	1.00	0.30
40% Microsized ZnO powder	0.00	0.00	0.00	4.00
30% SSF	2.00	2.00	3.50	2.00

foam. The use of nanosized materials of ZnO can impart additional properties apart from its primary application in the NRLF manufacturing process.

In this article, the synthesis and characterization of a ZnO-nanoparticle-incorporated NRLF matrix is explained. A modified NRLF and control NRLF were synthesized according to the well-known Dunlop manufacturing method, which is the most reliable and economical method of making NRLF since ancient times.[27] In our early research work, we found that the incorporation of silver nanoparticles could impart antibacterial and antifungal properties in the NRLF in a strong manner.[28,29] Apart from our previous research work, the research findings of this work would be the first to explain the enhancement of the antibacterial activities of NRLF through the incorporation of ZnO nanoparticles into the NRL compound. It would also be a very useful research area for other researchers to investigate more and more properties of these modified NRLF materials to use in many areas as well.

EXPERIMENTAL

Materials and Ingredients

NRL (low-ammonia type) and other rubber chemicals for making NRLF were supplied by Zarm Scientific and Supplies Sdn. Bhd. (Malaysia), and ZnO nanoparticles and chemicals for the antimicrobial susceptibility tests were obtained from Sigma Aldrich Chemicals. *Escherichia coli* (strain number NCTC 10418) and *Staphylococcus aureus* (SA; strain number NCTC 8532) strains were obtained from the Faculty of Dental Science, University of Peradeniya, Sri Lanka.

Compounding and Production of the ZnO-Nanoparticle-Incorporated NRLF Samples and Control Samples of NRLF

The formula used to make the NRLF by the Dunlop process is shown in Table I.[21] To make sample C [4 parts per hundred rubber (pphr) of nano-ZnO-incorporated NRLF], first, low-ammonia-type NRL was mixed with sulfur, the antioxidant, and potassium oleate soap with stirring at 10 rpm. After 2 h, zinc 2-mercaptobenzhiozolate (ZMBT) and zinc diethyldithiocarbamate (ZDEC) were slowly added to the mixture. Then compound mixer was matured for 8 h at room temperature with stirring at 10 rpm.

After maturation, the NRL compound mixture was vigorously beaten with a cake beater (Kenwood, kMix) to make a foam until the volume increased up to three times the initial volume. After that, 4.00-pphr 40% nanosized ZnO powder together with 0.30-pphr 40% DPG were added as the primary gelling agent to the foam, and beating was continued for another 90 s. Then, the secondary gelling agent, 2.00-pphr 30% sodium silicofluoride (SSF), was quickly added, and the mixture was beat for another 90 s. Finally, the ungelled foam was immediately poured into the aluminum mold and allowed to be gelled for 2 min at ambient temperature. The gelled NRLF was then cured in a hot-air oven at 100°C for 2 h. Next, the cured foam was stripped out from the mold and thoroughly washed with deionized water to remove the potassium oleate soap and nonreacted elements. After the cured NRLF was washed, it was dried in a hot-air oven at 80°C for 4 h. The resulting foam was off-white in color. The same procedure was carried out to make the control sample (sample A) without the addition of any ZnO particles, the 2-pphr nanosized-ZnO-incorporated sample (sample D), and the 4-pphr microsized-ZnO-incorporated sample (sample B) as per the formulations given in Table I.

Characterization

A transmission electron microscope was used to obtain the transmission electron microscopy (TEM) images (Philips CM12), and the images were analyzed with Docu version 3.2 image analysis.

X-ray diffraction (XRD; Bruker Analytical X-ray system, D8 ADVANCE) was used to obtain the XRD patterns of the commercial ZnO nanopowder and the modified NRLF.

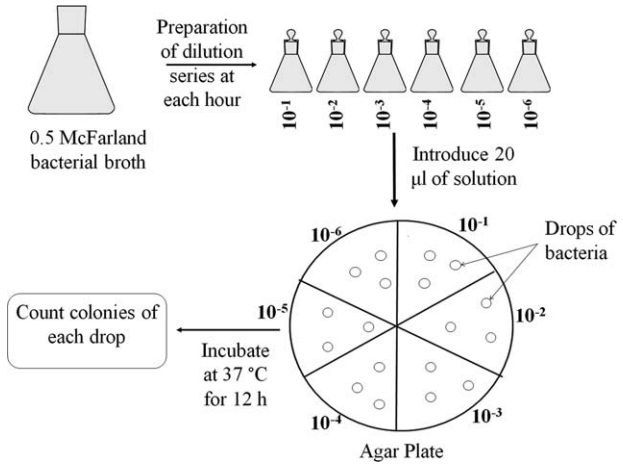

Figure 1. Graphical illustration of the Mile and Misra method.

A powder XRD technique with Cu Kα radiation was used to analyze the sample. The sample was scanned stepwise in the range $2\theta = 5–80°$ at a scanning rate of 0.001°/s.

A Zeiss Supra TM 35VP (Germany) operating at 10.00 kV and coupled with an EDAX Genesis instrument was used to analyze the scanning electron microscopy (SEM) images and energy-dispersive X-ray (EDX) analysis. The fractured surfaces of the foam rubber samples were coated with an alloy consisting of 80% gold and 20% palladium in a Bio-Rad Polaron Division SEM coating system.

Qualitative determination of the antimicrobial testing was done as described in following method. Luria Broth medium was prepared, and a single colony of Gram-positive SA was inoculated under aseptic conditions. SA-inoculated Luria Broth medium was then incubated at 37°C for 12 h in a mechanical shaker. After the incubation period, 100 μL of a 1×10^8 cfu/mL bacteria suspension was then added and evenly spread onto Muller Hinton agar plates. The modified and unmodified foam pieces with a size of 10×10 mm^2 were placed on the agar plates and aerobically incubated at 37°C for 24 h in an incubator. The antibacterial activity of the modified foam materials were assessed by the examination of a clear inhibition zone around the NRLF samples placed on agar plates. The same procedure was carried out for the Gram-negative *E. coli* bacteria as well.[30]

The quantitative determination of antimicrobial activity was done according to the Miles and Misra method.[31] Briefly, a single colony of the bacterial sample was inoculated into nutrient agar broth under aseptic conditions and was incubated at 37°C overnight in a mechanical shaker, and 30 mL of the sample of 0.5 McFarland equivalent broth was obtained. An NRLF sample with dimensions of 10×10 mm^2 was introduced to the broth and incubated at 37°C in a mechanical shaker during the experiment. Then, 1 mL of the bacterial solution was taken out at each 1-h interval, and a dilution series was prepared from 10^{-1} to and 10^{-6} under aseptic conditions to get a countable number of colonies per drop. Then, 20 μL of each of diluted solution was introduced onto the Muller Hinton agar plate as a single drop, and the plates were incubated at 37°C for 12 h. The results were triplicated, and colonies between 3 and 30 in a single drop were considered countable for each dilution (Figure 1). The sample was tested for a period of 0–6 h from the introduction of the foam sample to the original broth. The numbers of colonies present in each drop was equal to the number of bacterial cells alive in the broth at the time of removal of the 20 μL original sample. All of the colonies at each dilution was counted, averaged to get a value, and multiplied by the power of dilution to get the number present in the 20-μL original sample. The numbers of colonies were compared with the colonies of the controlled sample. Experiments were carried out for both Gram-negative *E. coli* and Gram-positive SA.[31]

RESULTS AND DISCUSSION

TEM Analysis of the ZnO Nanopowder

The TEM images taken from the commercial ZnO nanopowder dispersed in distilled water showed that most of the particles were below 100 nm [see Figure 2(a)]. The shapes of the particles could be clearly identified as spherical shapes and rodlike shapes in the enlarged view shown in Figure 2(b).

XRD Analysis of ZnO Nanopowder and NRLF Modified by Nano-ZnO

The XRD technique is most often used to determine crystal structures, crystal parameters, and sizes of crystallites. This technique is a very famous research tool among researchers who work on minerals and ceramics.[32,33] In our study, this important technique was used to prove the presence of the ZnO

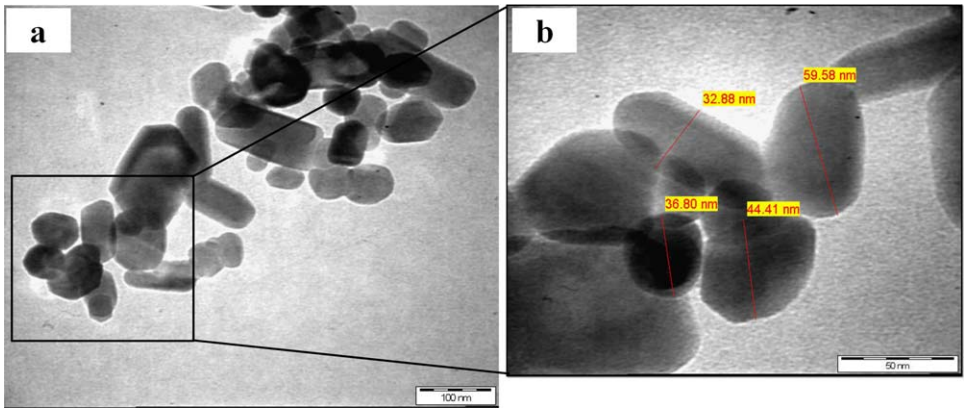

Figure 2. TEM microimage analysis of the ZnO nanoparticles at magnifications of (a) 13,000 and (b) 45,000×. [Color figure can be viewed in the online issue, which is available at wileyonlinelibrary.com.]

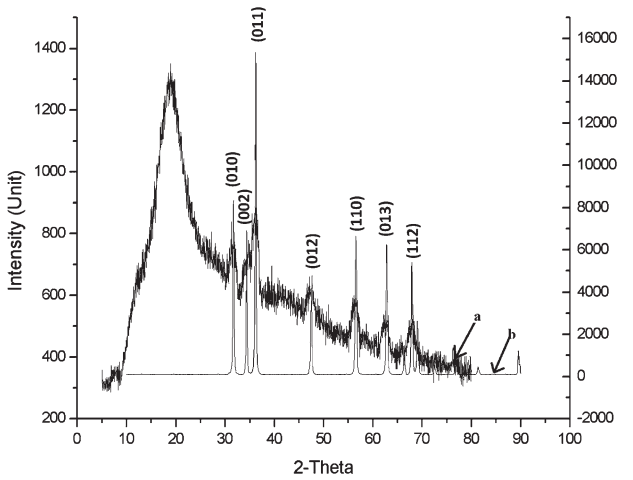

Figure 3. XRD spectra of the (a) NRLF modified by ZnO nanopowder and (b) commercial ZnO nanopowder.

crystal phase in the NRLF. It is very hard to obtain a prominent peak pattern for materials that have more amorphous phase than crystalline phase. However, according to the XRD peak pattern of the modified NRLF, we proved that the NRLF modified by ZnO nanopowder had clear peak patterns, which almost matched the peak patterns of the commercial ZnO nanopowder. The relative intensities in the XRD peaks of the ZnO commercial nanopowder perfectly matched with the reference code 98-002-6593, which was the hexagonal phase. The crystallite size calculated by the high expert software was 522.9 Å. Figure 3 shows that most of the peaks of the XRD pattern obtained for the 4-pphr nano-ZnO-incorporated NRLF matched with the XRD peaks of the commercial ZnO nanopowder. The reference code for the modified NRLF was 98-002-8868, which was also the hexagonal phase of the zincite compound. The XRD peaks obtained for the modified NRLF were not as prominent as they were for the pure ZnO nanopowder. The reason for this was that the NRLF was an amorphous material, and the mixed amount of the crystalline phase (nano-ZnO) was only 4 pphr. From the XRD results, we concluded that the modified NRLF had the crystalline phase of nano-ZnO.

Morphology of NRLF by SEM

Figure 4 shows the SEM micrographs of the fractured surface of sample C (4-pphr nano-ZnO-incorporated NRLF). At the higher magnification (50,000×), we observed that some particles on the surface of the NRLF matrix had particle sizes of 64, 80, and 91 nm. Then, the EDX analysis was carried out in this area to prove that the nanosized particles consisted of the Zn element. Because the nanosized ZnO particles were mixed with the compounded latex, it was hard to see the ZnO nanoparticles by SEM analysis on the matrix of the NRLF. It was proven from our previous studies on silver nanoparticles incorporated in NRLF that the SEM micrographs of surface-treated NRLF by silver nanoparticles showed a large number of nanosilver particles,[29] whereas when it was mixed with the NRL compound, it was very hard to see the nanosized particles in the NRLF matrix in SEM micrographs.[28]

EDX Analysis of the ZnO-Nanoparticle-Incorporated Foam

EDX is a good characterization technique for analyzing the presence of specific elements on a sample. Once the appearance of specific nanoparticles is detected via SEM micrograph analysis, EDX can be easily used to identify that specific element. The results of the EDX analysis of the 4-pphr ZnO-nanoparticle-incorporated NRLF (Figure 5) showed that the main percentage was carbon atoms (98.09 atom %, 93.46 w %). Carbon is the main element of cis-1,4-polyisoprene [$^{\wedge\wedge\wedge}CH_2{-}C(CH_3){=}CH{-}CH_2{}^{\wedge\wedge\wedge\wedge}$], which is the main repeating unit of NRL. Because the bare NRLF was not covered with any other stranger elements, it was obvious that the prominent peak of NRLF must have been for carbon. The atomic percentage and weight percentage of the Zn element were 0.66 and 3.42, respectively. Because ZnO was added to the NRL compound, the actual weight and atomic percentages could not be obtained from the EDX analysis, but it was very useful for proving that the detected particles from the SEM micrograph consisted of the Zn element.

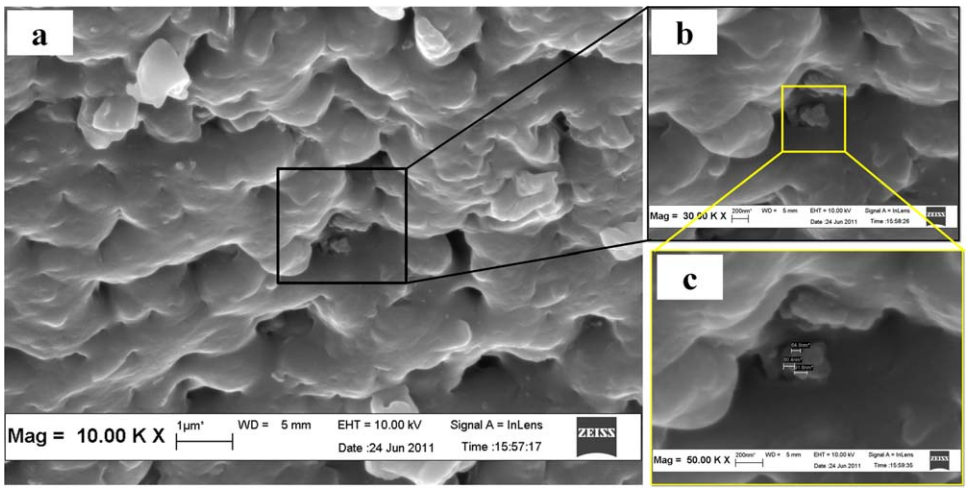

Figure 4. SEM images of NRLF treated with ZnO nanoparticles at (a) 10,000, (b) 30,000, and (c) 50,000×. [Color figure can be viewed in the online issue, which is available at wileyonlinelibrary.com.]

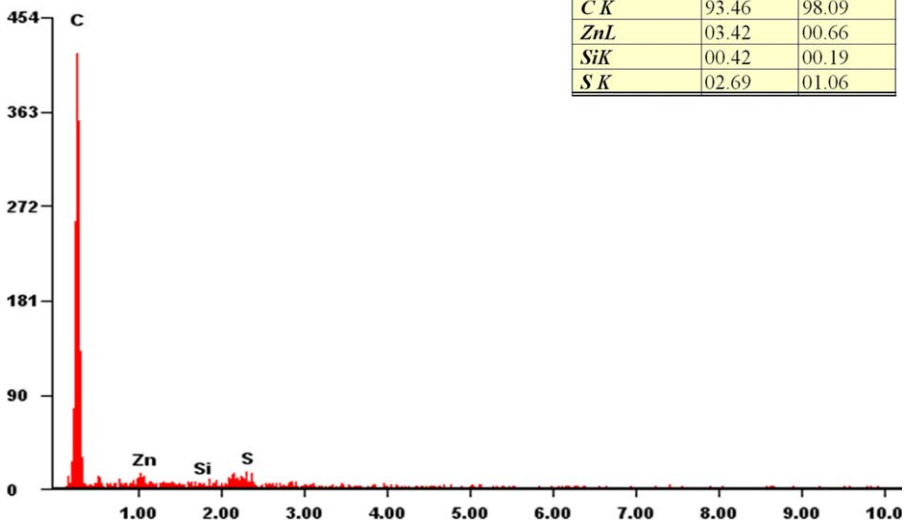

Element	Wt%	At%
C K	93.46	98.09
ZnL	03.42	00.66
SiK	00.42	00.19
S K	02.69	01.06

Figure 5. Elemental analysis of the modified NRLF. [Color figure can be viewed in the online issue, which is available at wileyonlinelibrary.com.]

Additives such as Si (from SSF) and sulfur used in the synthesis process of the NRLF could also be found in low percentages from the EDX analysis. However, other chemical additives used in the process of making compounded latex to make NRLF were hard to see in this analysis.

Testing of the Antibacterial Activity

The most important characteristics of the resulting NRLF were its antibacterial activities against two kinds of bacteria. Many researchers have reported the antibacterial activities of ZnO against Gram-negative *E. coli* bacteria. Dutta et al.[34] studied the effect of the size of ZnO nanoparticles on *E. coli*, the effect of light on the ZnO toxicity against *E. coli*, and also the toxic concentration of ZnO on *E. coli*. Studies done by Tam et al.[35] on the antibacterial activity of ZnO nanorods revealed that ZnO nanorods could damage the cell wall of *E. coli* bacteria and cause inhibition. Wahab et al.[36] reported that the minimum concentration of ZnO nanoparticles that could inhibit the growth of *E. coli* and SA was 15 μg/mL.

Results of the Qualitative Antibacterial Test. Figure 6(i) shows the antimicrobial activity of different samples against Gram-negative *E. coli*. Figure 6(ii) shows the antimicrobial activity of different samples against Gram-positive SA; it is clearly shown that the control sample (without ZnO) had no antibacterial activity against *E. coli*, whereas the highest activity (i.e., with a large diameter of the inhibition zone) was shown in sample D. The smaller sized inhibition zone belonged to sample C, whereas sample B had a moderate sized inhibition zone. The same results could be seen against Gram-positive SA; the

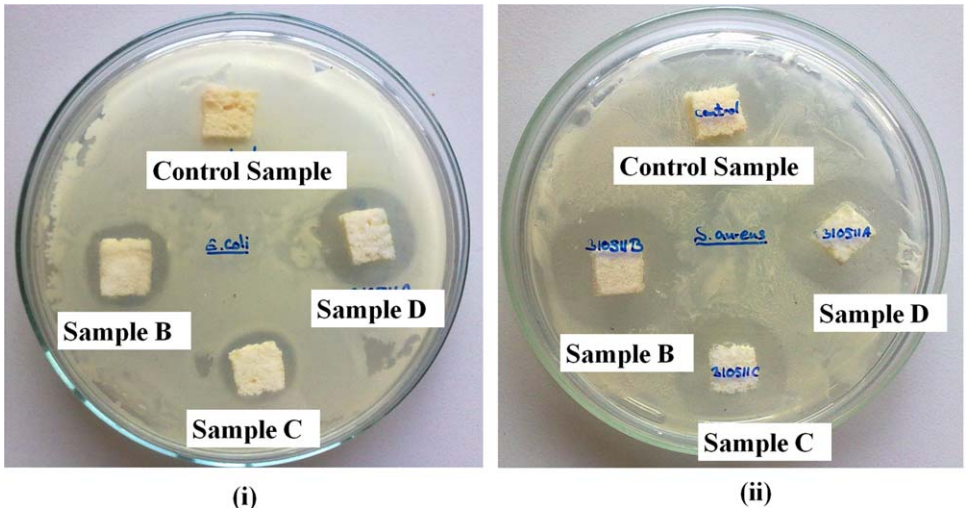

Figure 6. Testing of the qualitative antimicrobial activities against (i) Gram-negative *E. coli* [(B) 2-pphr nano-ZnO, (C) micro-ZnO, and (D) 4-pphr nano-ZnO] and (ii) Gram-positive SA [(B) 2-pphr nano-ZnO, (C) micro-ZnO, and (D) 4-pphr nano-ZnO]. [Color figure can be viewed in the online issue, which is available at wileyonlinelibrary.com.]

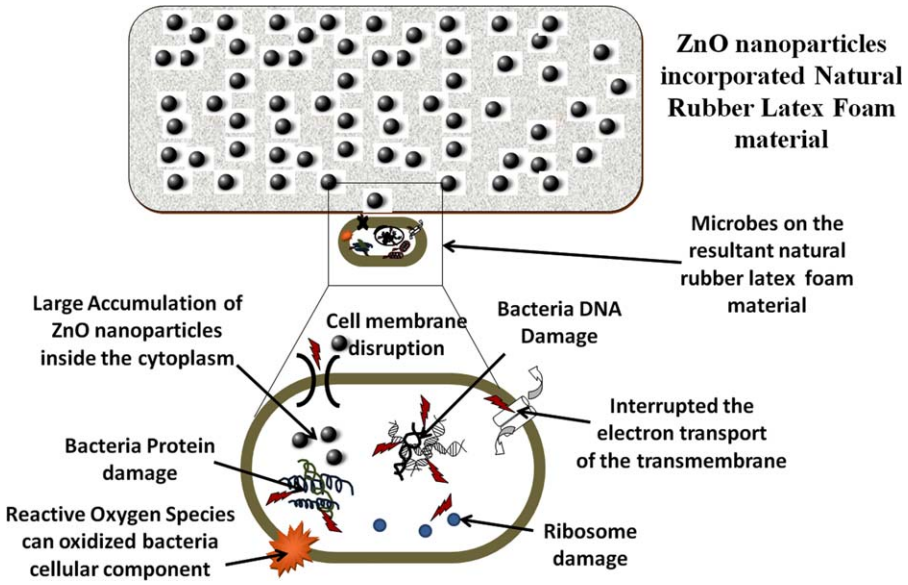

Figure 7. Possible mechanisms for killing bacteria from the modified NRLF. Adapted with permission from ref. 44. Copyright 2012 Reuters. [Color figure can be viewed in the online issue, which is available at wileyonlinelibrary.com.]

highest diameter of the inhibition zone belonged to sample D, and the lowest size of the inhibition zone belonged to the microsized ZnO-incorporated NRLF sample. The controlled sample had no inhibition zone. It was proven that the ZnO was the responsible element for the antibacterial activity of the NRLF matrix, and furthermore, it was proven that the nanosized ZnO had very good antibacterial activity against the two main groups of bacteria. In our previous research work, silver-nanoparticle-incorporated NRLF materials also showed good antimicrobial properties for the two main groups of bacteria. However, when we compared the sizes of inhibition zones, that of the nanosized-ZnO-incorporated NRLF was much greater than that of the silver-nanoparticle-incorporated NRLF.[28,29,37] In the literature, there are several reports by researchers who have tried to determine the real cause/causes of microorganism inhibition by ZnO nanoparticles.[38–40] Most researchers have found that the dominant factor for the killing of bacteria by nanosized ZnO could be the disintegration of the organic component of the bacteria by ROS produced on the surface of the ZnO nanostructures. Recently, this statement was further confirmed by many researchers investigating the possibility of killing several kinds of microorganisms from the ROS produced by ZnO nanostructures.[41,42] Zhang et al.[39] reported that the main cause for the killing of bacteria by nano-ZnO was the production of ROS. This finding was proven by Li et al.[43] in a detailed investigation of ROS produced by metal oxide nanoparticles. They found very interesting data on ROS production by several types of metal oxide nanoparticles. Among several types of metal oxide nanoparticles, nano-TiO_2 and nano-ZnO produced three types of ROS, called *superoxide radicals, hydroxyl radicals,* and *singlet oxygens*. They reported further that the antibacterial activity of the ZnO nanostructure on the *E. coli* bacterium was mainly due to this ROS production, and they also reported that the toxic Zn^{2+} ions had a low effect on the toxic properties. The liberation of Zn^{2+} ions from ZnO nanoparticles adsorbed on a solid NRLF matrix could be a difficult phenomenon, but it was easy to produce ROS through ZnO nanoparticles embedded on the NRLF matrix. Because the antimicrobial tests were performed under room light conditions, the most possible killing mechanism of bacteria from the modified NRLF samples by ZnO nanoparticles was the disintegration of the organic compound by ROS produced by the surface of the ZnO nanostructures. However, all of the possible killing mechanisms of bacteria from the modified NRLF are illustrated in Figure 7. Further studies are in progress to identify the exact reason or reasons for the killing mechanism of bacteria by the modified

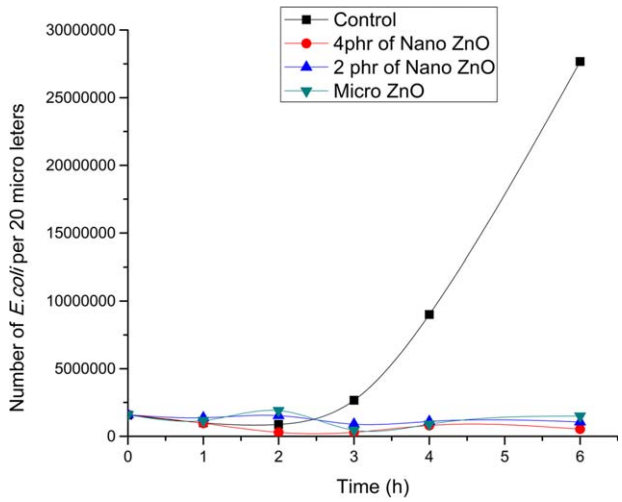

Figure 8. Growth of *E. coli* with time. [Color figure can be viewed in the online issue, which is available at wileyonlinelibrary.com.]

Table II. Comparison of the Growth of SA in the Presence of the Modified NRLF with Time

	Number of SA colonies per 20 μL			
Time (h)	Control	4-pphr Nano-ZnO	2-pphr Nano-ZnO	Micro-ZnO
0	10,330	10,330	10,330	10,330
1	190,000	6,330	66,600	16,330
2	1,267,000	4,660	62,340	1,330
3	2,500,000	733	2670	1,400
4	4,000,000	123	660	3,330
6	7,667,000	63	260	5,660

NRLF materials under several conditions, including dark, UV light, and direct sunlight conditions.

Results of the Quantitative Antibacterial Testing. Observations from the qualitative antibacterial tests were also proven by the quantitative antibacterial tests. Figure 8 shows the comparison between the inhibition of *E. coli* bacteria by each sample and that of the control sample with time. It clearly shows that the number of *E. coli* colonies decreased gradually with time because of the antibacterial activities of the modified samples. Sample D (4-pphr nano-ZnO-incorporated NRLF) had the highest efficiency, whereas the lowest activity was shown by the 4-pphr micro-ZnO-incorporated sample (sample C). The control sample did not show any antibacterial activity, as it showed high amount of bacterial growth as time passed.

In Table II, a similar trend is shown for SA as well. In the control sample, the number of bacterial colonies increased enormously, as it did not show any antimicrobial activity. In both the 4- and 2-pphr samples, the number of colonies decreased gradually due to the antibacterial activity, and the 4-pphr sample had the highest activity. As the micro-ZnO had a lesser activity compared to the 2- and 4-pphr nano-ZnO-incorporated NRLF samples, the reduction was not as effective as in the latter two, even though it was far better than the control sample. The highest surviving density was found in the control sample of the NRLF; the colony density was 700 times greater than the initial density because of the growth of SA. In all other samples, the density was decreased because of the antibacterial activity of ZnO. The greatest decrease in the colony density was shown in the NRLF sample with 4-pphr nano-ZnO because of its antimicrobial activity. After 6 h, 63, 260, and 5660 cells per 20 μL survived in the 4-pphr nano-ZnO-, 2-pphr nano-ZnO-, and 4-pphr micro-ZnO-incorporated NRLF, respectively; the initial broth contained 10,330 cells per 20 μL. These quantitative results confirmed that the nanosized-ZnO-incorporated NRLF showed very good antibacterial activities compared to the microsized-ZnO-incorporated NRLF matrix. It was also proven that ZnO was the responsible element for the antibacterial activity of the NRLF matrix.

CONCLUSIONS

From the results obtained, we concluded that ZnO was the main responsible material for the antimicrobial activity of NRLF. Also, we found that the incorporation of nanosized ZnO increased the antibacterial activity in a very strong manner, and it was proven that the resulting NRLF could inhibit Gram-negative *E. coli* and Gram-positive SA. Furthermore, the amount of antibacterial activity depended on the quantity of nanosized ZnO presence in the NRLF matrix as well. Finally, we concluded that the antibacterial activities of the microsized-ZnO-incorporated NRLF was increased significantly with the incorporation of nanosized ZnO in to the NRLF matrix. Furthermore, the modified NRLF by nanosized ZnO could be used as an antibacterial NRLF product wherever antibacterial foam materials are needed.

ACKNOWLEDGMENTS

This study was supported by a research university grant (contract grant number 1001/PBAHAN/814129). Universiti Sains Malaysia is gratefully acknowledged by one of the authors for the financial support of his Ph.D. studies. W. G. I. U. Rathnayake has received the grant for his Ph.D studies.

REFERENCES

1. Stoimenov, P. K.; Klinger, R. L.; Marchin, G. L.; Klabunde, K. *J. Langmuir* **2002**, *18*, 6679.
2. Ravishankar Rai, V.; Bai, J. In Science Against Microbial Pathogens: Communicating Current Research and Technological Advances; Mendez-Vilas, A., Ed.; University of Mysore: Mysore, India, **2011**; p 197.
3. Klingshirn, C. F.; Meyer, B. K.; Waag, A.; Hoffmann, A.; Geurts, J. M. M. Zinc Oxide: From Fundamental Properties Towards Novel Applications; Springer-Verlag: Berlin, **2010**.
4. Vigneshwaran, N.; Kumar, S.; Kathe, A.; Varadarajan, P.; Prasad, V. *Nanotechnology* **2006**, *17*, 5087.
5. Yadav, A.; Prasad, V.; Kathe, A.; Raj, S.; Yadav, D.; Sundaramoorthy, C.; Vigneshwaran, N. *Bull. Mater. Sci.* **2006**, *29*, 641.
6. Li, Q.; Mahendra, S.; Lyon, D. Y.; Brunet, L.; Liga, M. V.; Li, D.; Alvarez, P. J. *J. Water Res.* **2008**, *42*, 4591.
7. Perelshtein, I.; Applerot, G.; Perkas, N.; Wehrschetz-Sigl, E.; Hasmann, A.; Guebitz, G.; Gedanken, A. *Am. Chem. Soc. Appl. Mater. Interfaces* **2008**, *1*, 361.
8. Li, X.; Xing, Y.; Jiang, Y.; Ding, Y.; Li, W. *Int. J. Food Sci. Technol.* **2009**, *44*, 2161.
9. Rajendra, R.; Balakumar, C.; Ahammed, H. A. M.; Jayakumar, S.; Vaideki, K.; Rajesh, E. *Int. J. Eng. Sci. Technol.* **2010**, *2*, 202.
10. Sawai, J.; Shoji, S.; Igarashi, H.; Hashimoto, A.; Kokugan, T.; Shimizu, M.; Kojima, H. *J. Ferment. Bioeng.* **1998**, *86*, 521.
11. Applerot, G.; Lipovsky, A.; Dror, R.; Perkas, N.; Nitzan, Y.; Lubart, R.; Gedanken, A. *Adv. Funct. Mater.* **2009**, *19*, 842.
12. Zhang, L.; Jiang, Y.; Ding, Y.; Daskalakis, N.; Jeuken, L.; Povey, M.; O'Neill, A. J.; York, D. W. *J. Nanopart. Res.* **2010**, *12*, 1625.
13. Brayner, R.; Ferrari-Iliou, R.; Brivois, N.; Djediat, S.; Benedetti, M. F.; Fiévet, F. *Nano Lett.* **2006**, *6*, 866.

14. Huang, Z.; Zheng, X.; Yan, D.; Yin, G.; Liao, X.; Kang, Y.; Yao, Y.; Di Huang, A.; Hao, B. *Langmuir* **2008**, *24*, 4140.
15. Jones, N.; Ray, B.; Ranjit, K. T.; Manna, A. C. *FEMS Microbiol. Lett.* **2008**, *279*, 71.
16. Roberts, A. D. Natural Rubber Science and Technology; Oxford University Press: Oxford, United Kingdom, **1988**.
17. Murphy, E. *Ind. Eng. Chem.* **1952**, *44*, 756.
18. Blackley, D. C. Polymer Latices: Science and Technology, Chapman & Hall: London, **1997**.
19. Petri, C. Latex 2004: The 3rd Two-Day Conference on Synthetic Emulsions, Natural Latex and Latex Based Products, iSmithers Rapra Publishing, Hamburg, Germany, 20–21 April 2004; **2004**; p 47.
20. Riyajan, S. A.; Santipanusopon, S.; Yai, H. KGK Kautsch. *Gummi Kunstst.* **2010**, *63*, 6.
21. Madge, E. W. Latex Foam Rubber; Maclaren and Sons Ltd: London, **1962**.
22. Calvert, K.; Applied Science Publishers Ltd., London, England, **1982**.
23. Coleman, V.; Jagadish, C. In Zinc Oxide Bulk, Thin Films and Nanostructures; Jagadish, C., Pearton, S., Eds.; Elsevier: Amsterdam, **2006**; Chapter 1.
24. Becheri, A.; Dürr, M.; Lo Nostro, P.; Baglioni, P. *J. Nanopart. Res.* **2008**, *10*, 679.
25. Nair, S.; Sasidharan, A.; Divya Rani, V.; Menon, D.; Manzoor, K.; Raina, S. *J. Mater. Sci.: Mater. Med.* **2009**, *20*, 235.
26. Banoee, M.; Seif, S.; Nazari, Z. E.; Jafari-Fesharaki, P.; Shahverdi, H. R.; Moballegh, A.; Moghaddam, K. M.; Shahverdi, A. R. *J. Biomed. Mater. Res. Part B* **2010**, *93*, 557.
27. Madge, E. W. U.S. Patent No. 2,200,847. Washington, DC: U.S. Patent and Trademark Office, **1940**.
28. Rathnayake, W.; Ismail, H.; Baharin, A.; Darsanasiri, A.; Rajapakse, S. *Polym. Test.* **2012**, *31*, 586.
29. Rathnayake, I.; Ismail, H.; Azahari, B.; Darsanasiri, N. D.; Rajapakse, S. *Polym.-Plast. Technol. Eng.* **2012**, *51*, 605.
30. Cockerill, F. R.; Wikler, M.; Bush, K.; Dudley, M.; Eliopoulos, G.; Hardy, D. Clinical and Laboratory Standards Institute. Performance standards for antimicrobial susceptibility testing: twentieth informational supplement. 20th ed. Wayne: Clinical and Laboratory Standards Institute, **2010**.
31. Miles, A.; Misra, S.; Irwin, J. *J. Hyg.* **1938**, *38*, 732.
32. Stanjek, H.; Häusler, W. *Hyperfine Interact.* **2004**, *154*, 107.
33. Hope, H. *Prog. Inorg. Chem.* **1994**, *41*, 1.
34. Dutta, R. K.; Sharma, P. K.; Bhargava, R.; Kumar, N.; Pandey, A. C. *J. Phys. Chem. B* **2010**, *114*, 5594.
35. Tam, K.; Djurišić, A.; Chan, C.; Xi, Y.; Tse, C.; Leung, Y.; Chan, W.; Leung, F.; Au, D. *Thin Solid Films* **2008**, *516*, 6167.
36. Wahab, R.; Mishra, A.; Yun, S. I.; Kim, Y. S.; Shin, H. S. *Appl. Microbiol. Biotechnol.* **2010**, *87*, 1917.
37. Rathnayake, W.; Ismail, H.; Azahari, B.; Bandara, I.; Rajapakse, S. *Polym.-Plast. Technol. Eng.*, to appear.
38. Xia, T.; Kovochich, M.; Liong, M.; Mädler, L.; Gilbert, B.; Shi, H.; Yeh, J. I.; Zink, J. I.; Nel, A. E. *ACS Nano* **2008**, *2*, 2121.
39. Zhang, L.; Jiang, Y.; Ding, Y.; Daskalakis, N.; Jeuken, L.; Povey, M.; O Neill, A. J.; York, D. W. *J. Nanopart. Res.* **2010**, *12*, 1625.
40. Yin, H.; Casey, P. S.; McCall, M. J.; Fenech, M. *Langmuir* **2010**, *26*, 15399.
41. Dutta, R. K.; Nenavathu, B. P.; Gangishetty, M. K.; Reddy, A. V. R. *Colloids Surf. B* **2012**, *94*, 143.
42. Guo, D.; Bi, H.; Liu, B.; Wu, Q.; Wang, D.; Cui, Y. *Toxicol. In Vitro*, to appear.
43. Li, Y.; Zhang, W.; Niu, J.; Chen, Y. *ACS Nano* **2012**, *6*, 5164.
44. Hajipour, M. J.; Fromm, K. M.; Akbar Ashkarran, A.; Jimenez de Aberasturi, D.; Larramendi, I. R. D.; Rojo, T.; Serpooshan, V.; Parak, W. J.; Mahmoudi, M. *Trends Biotechnol.*, to appear.